National Park Service
U.S. Department of the Interior

Natural Resource Stewardship and Science

Stability of Ice-Wedges in Kobuk Valley National Park and the Noatak National Preserve, 1951-2009

Natural Resource Report NPS/ARCN/NRR—2016/1248

ON THE COVER

Narrow ponds due to degradation of ice wedges surround a high-center ice-wedge polygon in the Ahnewetut Wetlands of Kobauk Valley National Park, Alaska. Photo by the author on 2 August 2012, latitude 67.096 longitude -158.551

Stability of Ice-Wedges in Kobuk Valley National Park and the Noatak National Preserve, 1951-2009

Natural Resource Report NPS/ARCN/NRR—2016/1248

David K. Swanson

National Park Service
4175 Geist Road
Fairbanks, AK 99708

July 2016

U.S. Department of the Interior
National Park Service
Natural Resource Stewardship and Science
Fort Collins, Colorado

The National Park Service, Natural Resource Stewardship and Science office in Fort Collins, Colorado, publishes a range of reports that address natural resource topics. These reports are of interest and applicability to a broad audience in the National Park Service and others in natural resource management, including scientists, conservation and environmental constituencies, and the public.

The Natural Resource Report Series is used to disseminate comprehensive information and analysis about natural resources and related topics concerning lands managed by the National Park Service. The series supports the advancement of science, informed decision-making, and the achievement of the National Park Service mission. The series also provides a forum for presenting more lengthy results that may not be accepted by publications with page limitations.

All manuscripts in the series receive the appropriate level of peer review to ensure that the information is scientifically credible, technically accurate, appropriately written for the intended audience, and designed and published in a professional manner.

This report received formal peer review by subject-matter experts who were not directly involved in the collection, analysis, or reporting of the data, and whose background and expertise put them on par technically and scientifically with the authors of the information.

Views, statements, findings, conclusions, recommendations, and data in this report do not necessarily reflect views and policies of the National Park Service, U.S. Department of the Interior. Mention of trade names or commercial products does not constitute endorsement or recommendation for use by the U.S. Government.

This report is available in digital format from the National Park Service, Arctic Inventory and Monitoring Network (http://science.nature.nps.gov/imn/units/arcn), and the Natural Resource Publications Management website (http://www.nature.nps.gov/publications/nrpm/). To receive this report in a format optimized for screen readers, please email irma@nps.gov**.**

Please cite this publication as:

Swanson, D. K. 2016. Stability of ice-wedges in Kobuk Valley National Park and the Noatak National Preserve, 1951-2009. Natural Resource Report NPS/ARCN/NRR—2016/1248. National Park Service, Fort Collins, Colorado.

NPS 187/133533, 189/133533, July 2016

Contents

Contents (continued)

Figures

Tables

Abstract

Ice-wedge polygons are characteristic arctic landforms that are vulnerable to change in a warming climate. Degradation of ice wedges causes subsidence along the margins of ice-wedge polygons, which can produce small ponds that are visible on remotely sensed images. Ice-wedge polygons are common in the Ahnewetut Wetlands of Kobuk Valley National Park (AHN) and the Lower Noatak Lowlands of the Noatak National Preserve (LNL) in northwestern Alaska. I placed 300 random 1-ha plots in each of these regions on images from 1951-1952 and 2006-2009, and mapped surface water present within the portions of the plots occupied by ice-wedge polygons. The absolute area of small ponds was difficult to compare between image dates due to differences in image quality and potential short-term variations in wetness of the landscape. Thus I used the distribution of water relative to ice-wedge polygon centers as a measure of ice-wedge degradation. I mapped water by thresholding panchromatic images (pixels darker than the threshold were classified as water) and then computed the distance index $2a/(a+b)$ for each water pixel, where a and b are the distances to the nearest and second nearest polygon centers, respectively. This index ranges from near zero at polygon centers to near one at polygon margins, and thus can be used to analyze the location of water within the ice-wedge polygons.

In the AHN study area, water was concentrated near polygon centers in 1951-52 and on polygon margins in 2006-2009, due to the appearance of numerous water-filled troughs over degraded ice wedges. The proportion of polygons with marginal ponds, indicating ice-wedge degradation, increased from 7% to 22% between the two time periods. Visual assessment of the plots confirmed that new polygon-marginal ponds formed between the image dates. In the LNL study area, water along polygon margins was more prevalent in 2006-2008 than 1951, but the change was not as marked as in the AHN study area: in 1951, 9% of the polygons had marginal ponds, while in 2006-08 this proportion had increased to 12%. Reasons for the greater amount of ice-wedge degradation in the AHN study area are unclear, but it may be due to AHN's position near the warm climatic limit for ice wedge development or its different topographic setting. A 1977 fire in the LNL study area had no effect on the prevalence of polygon-marginal ponds there in 2006-08. Continued ice-wedge degradation is expected in both study areas as a result of recent climate warming.

Acknowledgments

Thanks to Jon O'Donnell and Ben Jones for helpful review comments.

List of Terms and Acronyms

Active layer. Ground above *permafrost* that thaws each summer.

AHN. Ahnewetut Wetlands subsection in Kobuk Valley National Park.

ARCN. The NPS Arctic Inventory and Monitoring Network.

Color-infrared. Refers to images that contain data from visible light and the near infrared wavelength bands (invisible to the human eye, with wavelengths longer than those of red color). To enable printing or screen projection of these images by a red-green-blue color scheme, the infrared, red, and green data are portrayed using red, green, and blue colors, respectively.

Epigenetic. Refers to ice wedges that formed after deposition of the enclosing material was complete (van Everdingen 1998). Contrasts with *syngenetic*.

High-center ice-wedge polygon. Ice-wedge polygon with high center sloping out to a lower marginal trough, often but not always produced by degradation of ice wedges.

Ice wedges. Ground ice formed by contraction cracking of frozen ground in the winter followed by infilling with water that freezes and is preserved in permafrost. The surface manifestation of actively growing ice wedges as viewed from above is ice-wedge polygons.

Holocene. The most recent geologic epoch, extending from 11,700 years ago to the present (Cohen et al. 2013). The Holocene was a time of relatively stable warm climate, after the last Pleistocene glacial episode.

IKONOS. A commercial satellite that collected multispectral (multiple wavelengths of light) imagery with 4-m resolution that can be pan-sharpened (enhanced using higher-resolution panchromatic data) to 1-m resolution.

KOVA. Kobuk Valley National Park.

LNL. Lower Noatak Lowlands subsection in the Noatak National Preserve.

Low-center ice wedge polygon. Ice-wedge polygon with central depression and low ridges along the polygon margins.

NOAT. Noatak National Preserve.

NPS. National Park Service

Permafrost. Ground that remains below 0° C for two or more consecutive years. In ARCN most permafrost has been frozen for thousands of years and is many meters thick.

Pleistocene. The geologic epoch extending from 2.58 million to 11,700 years ago and characterized by multiple cold periods known informally as "ice ages" (Cohen et al. 2013).

Subsection. Short for "ecological subsection", a unit of terrain in the National Hierarchical Framework of Ecological Units (Cleland et al. 1997).

Syngenetic. Refers to ice wedges that formed in material as it was accumulating. Syngenetic ice wedge grow upward as material accumulates and thus reach greater vertical dimensions than *epigenetic* ice wedges (van Everdingen 1998).

Thaw degree-days. Sum of daily positive temperatures (in degrees C) through the year.

Thermokarst. Subsidence due to thaw of ice in the ground.

Introduction

Ice-wedge polygons are a striking and widespread feature of the arctic landscape. They form when frozen ground cracks due to contraction in the winter, the cracks fill with ice, and the resulting wedge of ice is preserved in permafrost (Leffingwell 1915, Lachenbruch 1963). After many years of cracking in approximately the same place, ice wedges can become a meter or more wide at the top. These ice wedges are vulnerable to thaw because they are nearly pure ice bodies near the surface, with little insulating overlying material. Surface disturbance or a warming climate can cause them to thaw and produce surface subsidence. Jorgenson et al. (2006), Jones et al. (2015), Jorgenson et al (2015), and Liljedahl et al. (2016) have reported significant degradation of ice wedges on the North Slope of Alaska in recent decades. Necsoiu et al. (2013) reported ice-wedge degradation in a small study area in Kobuk Valley National Park. Because of the sensitivity of ice wedges to thaw, ice-wedge polygon monitoring is a part of the permafrost monitoring program for the National Park Services Arctic Inventory and Monitoring Network (ARCN, the five National Park units in northern Alaska). The present study was carried out as a part of ARCN permafrost monitoring.

Actively growing ice-wedge polygons typically have a low ridge, on both sides of the wedge,that is higher than the polygon center, hence the name "low-center ice wedge polygon" (van Everdingen 1998). In poorly drained permafrost lowlands, low-center polygons often have wet soils or standing water in the polygon centers, ringed by the higher margins, and a narrow wet trench centered over the wedge (Fig. 1).

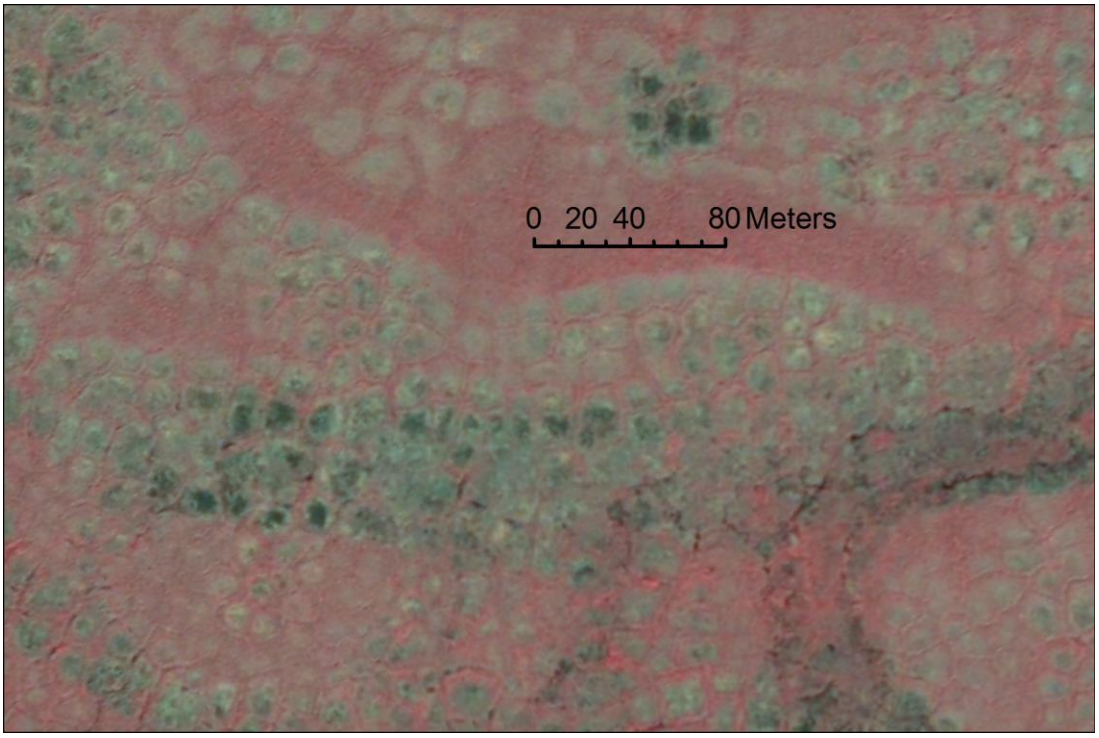

Figure 1. Low-center polygons in the Lower Noatak Lowlands. The low centers of these polygons are darker than the margins because they have shallow ponded water and less vegetation. IKONOS image, 3 July 2007, color-infrared color scheme.

When an ice wedge melts, subsidence occurs over and adjacent to the wedge, i.e. around the polygon margin. A polygon where the wedge has melted due to thaw of permafrost typically has small oblong ponds over the degraded wedges; larger ponds sometimes form at wedge junctions (Fig. 2). Subsidence due to thaw of ground ice is called thermokarst (Czudek and Demek 1970). Subsidence along the wedges often results in high-center ice-wedge polygons (van Everdingen 1998; Fig. 3). High-center polygons are driest in the center and wetter around the margins. Initial ice-wedge degradation results in high-center polygons with disconnected ponds in the marginal troughs; with continued degradation the ponds may become connected and increase surface runoff (Liljedahl et al. 2016).

Figure 2. An example of a small pond formed by ice-wedge degradation in the Ahnewetut Wetlands ecological subsection of KOVA. Elongated ponds form over degraded ice wedges, these are about 1 m wide and several meters long. Right-angle intersections such as this one are common.

Polygons without a marginal ridge can develop on dry sites with deep active layers where there is little ice accumulation in wedges in the permafrost (Romanovskiy 1977). These polygons can be high-centered, and thus not all high-center polygons should be assumed to result from ice-wedge degradation. However, ponding is minimal in these situations due to good drainage.

Ice wedges may be epigenetic (formed in material after deposition ceased) or syngenetic (formed in material during deposition; van Everdingen 1998). Syngenetic ice wedges that formed as a result of silt deposition by wind during the Pleistocene are present in parts of ARCN; they can extend to great

depths (Shur 2009) and may have no obvious surface expression. The present study was carried out in areas dominated by active, epigenetic ice wedges that are clearly visible at the surface.

Figure 3. Ice-wedge polygons in the Lower Noatak Lowlands, Noatak National Preserve. Note the person wearing an orange vest, for scale. The polygons in the vicinity of the person are high-center polygons, with wet, sedge-dominated margins and drier centers with low shrubs.

The presence or absence of ponds formed by ice-wedge degradation can be determined by analysis of high-resolution aerial photographs and satellite images (Jorgenson et al. 2006, Liljedahl et al. 2016). Wet areas with tundra vegetation are readily visible as darker tones on images. The present report assesses the degradation of ice wedges in 2 study areas in ARCN by mapping surface water within ice-wedge polygon perimeters. The absolute area of water in polygon vicinities is difficult to determine precisely, due to overlap in the appearance of saturated peaty soils, shallow water over vegetation, and shallow water with floating or emergent vegetation. Thus I analyzed the location of water within polygons – on margins vs. in centers – rather than the absolute area of water cover to assess ice-wedge polygon degradation.

Methods

Study Areas

Ahnewetut Wetlands, Kobuk Valley National Park

Kobuk Valley National Park (KOVA) occupies about 7100 square kilometers in the lowlands along the Kobuk River and adjacent mountains. Ice wedge polygons with visible surface manifestations are not widespread in KOVA. They occur almost exclusively in the Ahnewetut Wetland ecological subsection (Fig. 4, Swanson 2001). The Ahnetwetut Wetlands are a region of numerous lakes with wetlands in between, on sandy sediments near the Great Kobuk Sand Dunes (Figs. 5 and 6). While the lowlands in KOVA are mostly forested, the wetland areas with permafrost and thin active layers where ice-wedge polygons occur are mostly treeless. Ice wedges are generally inactive or weakly active, and thus quite inconspicuous, in the forested environments of Interior Alaska; ice wedges are active in arctic Alaska, with the transition occurring near the Ahnewetut study area (Pewe 1975, Jorgenson et al. 2008). The Ahnetwetut Wetlands ice-wedge polygon field is the last dense network of ice-wedge polygons with clear surface manifestation that one observes when flying to the south and east in this part of the Kobuk Valley, suggesting that these wedges are near the recent climatic limit of active ice-wedge growth.

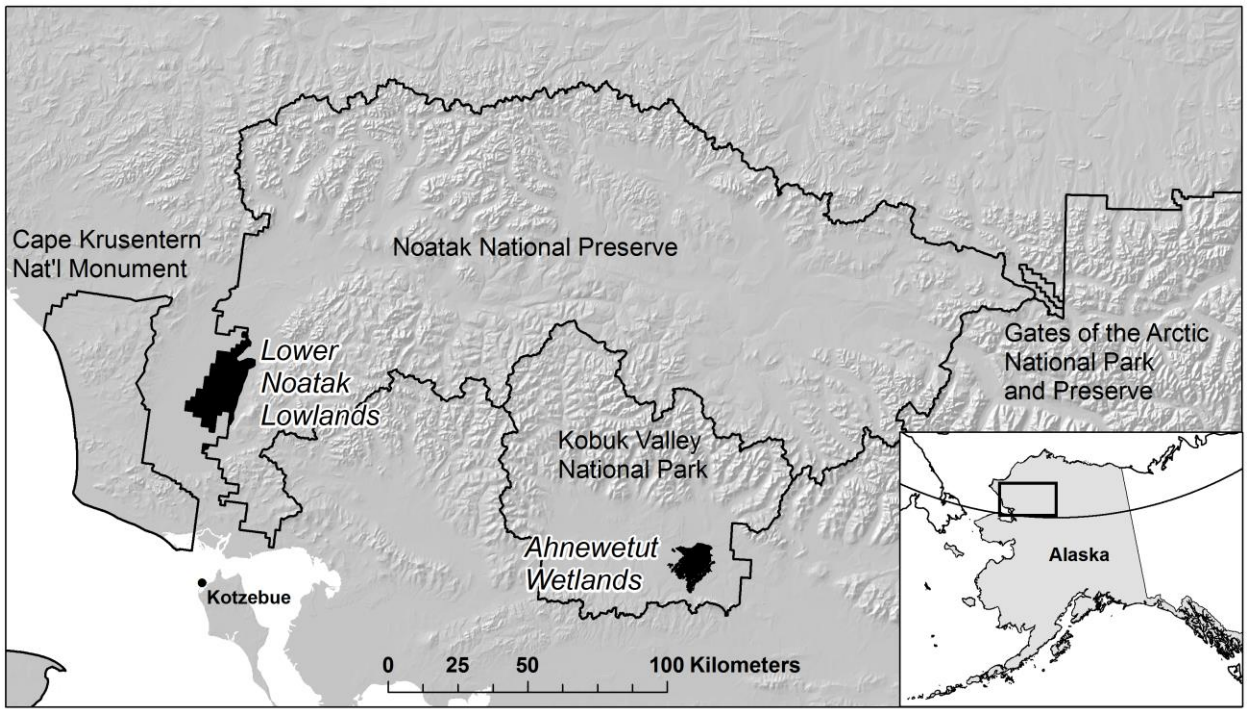

Figure 4. Location of the two study areas: the Ahnewetut Wetlands in Kobuk Valley National Park and the Lower Noatak Lowlands in the Noatak National Preserve.

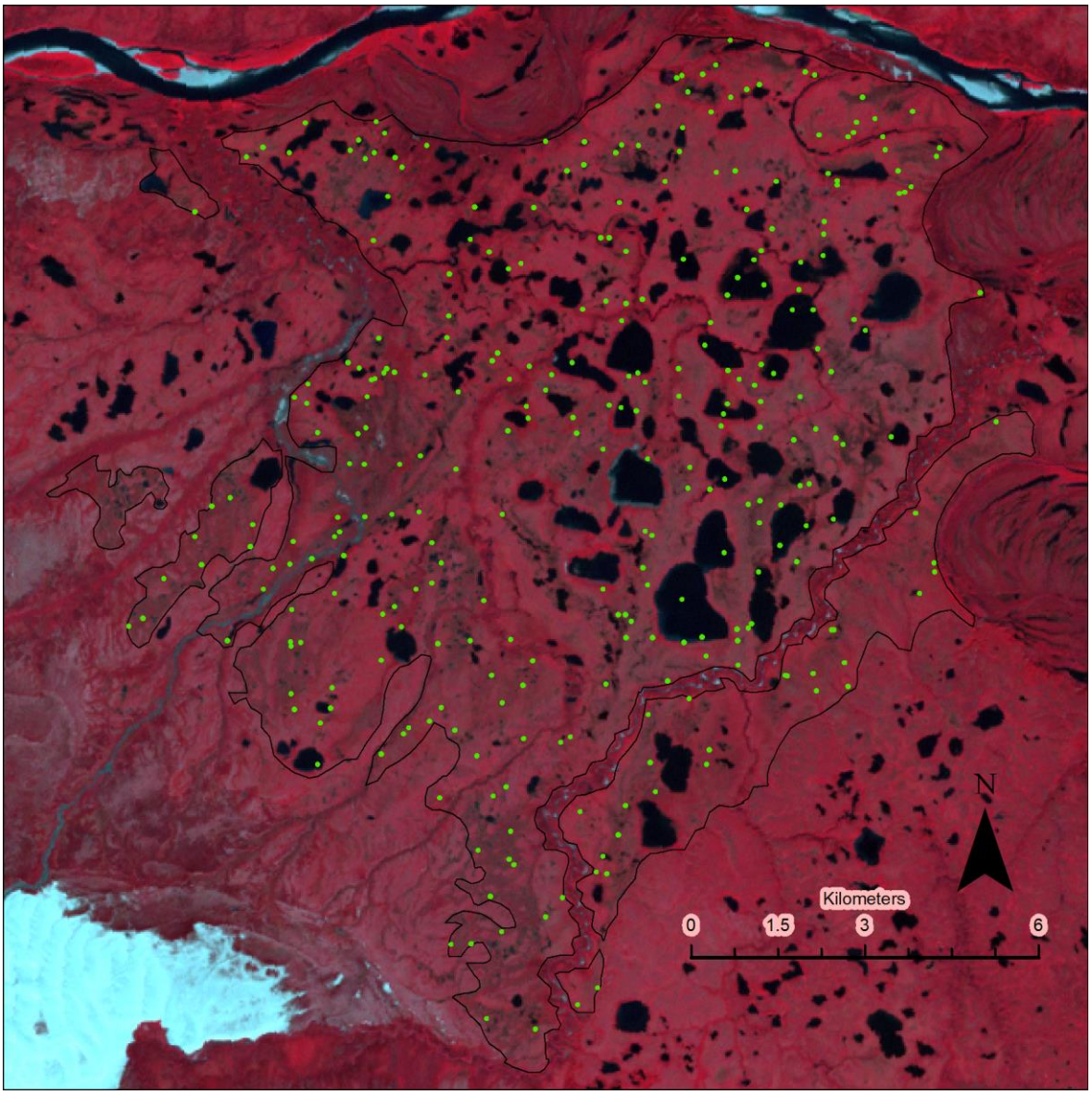

Figure 5. Overview of the Ahnewetut Wetlands study area in Kobuk Valley National Park. The Ahnewetut Wetlands subsection is outlined in black, and green dots mark remotely sensed plot locations. The large gaps between plots in the central part of the study are places where random plots were dropped due to clouds on the IKONOS images. The white area southwest of the study area is the Great Kobuk Sand Dunes. The background image here is a Landsat mosaic from the early 2000s, displayed in a color-infrared color scheme.

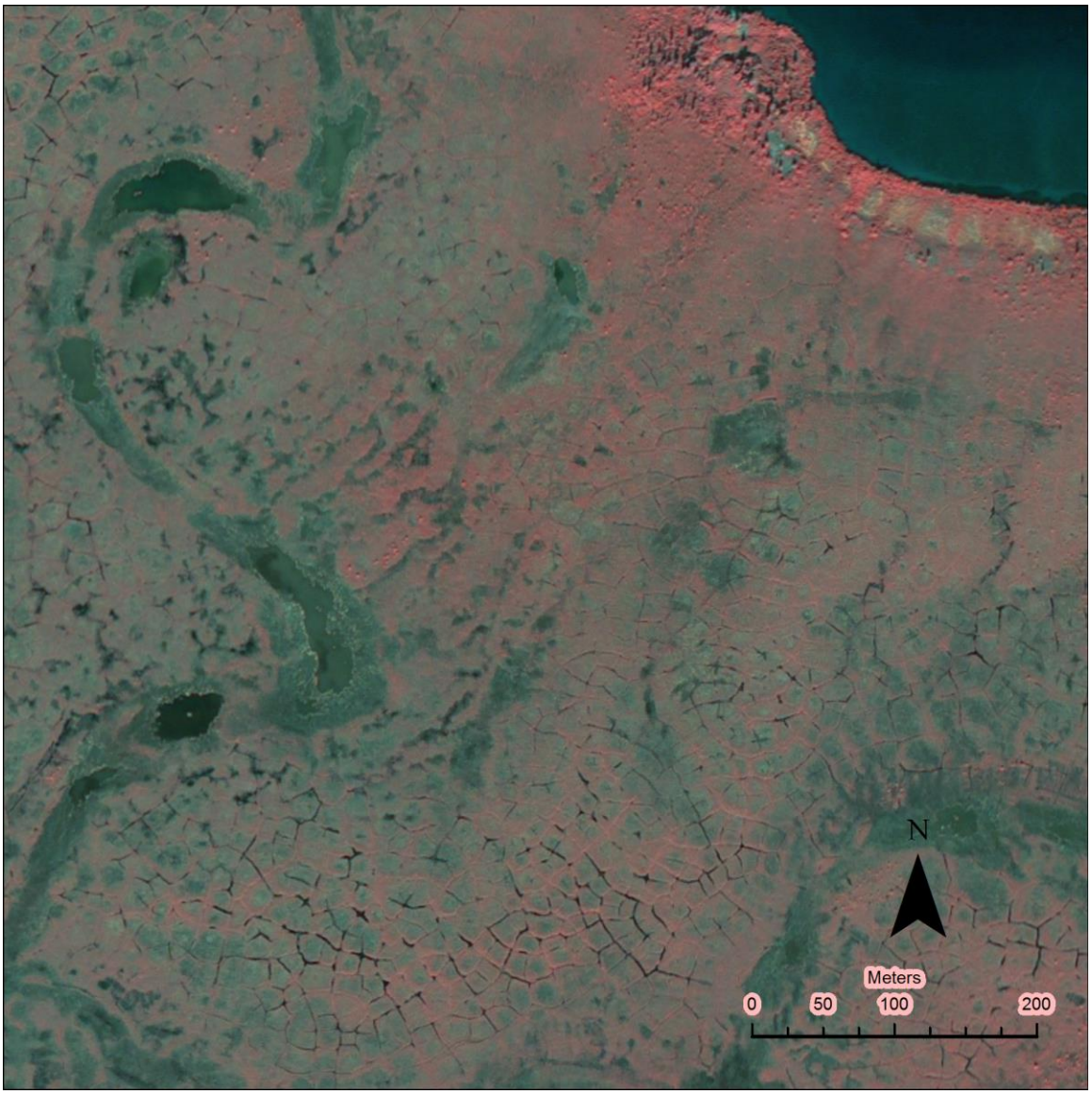

Figure 6. Landscape of the Ahnewetut Wetlands study area. Numerous narrow ponds from degradation of ice wedges are visible in the southern part of this IKONOS image from 10 August 2007. The sinuous feature with larger ponds along the west side of the photo is a former stream channel. Tall shrub vegetation with a few spruce trees casting shadows is visible near the large lake in the northeast.

Twelve soil pits dug in ice-wedge polygon terrain near the center of the Ahnewetut Wetlands as a part of another study (Swanson 2013) between 31 July and 2 Aug 2012 were frozen at depths ranging from 36 to 80 cm, and most had water within 30 cm of the surface. Six of these pits had organic soil material (peat) down to the frozen layer, and the other six had sandy sediments under 30-45 cm of peat. Vegetation consisted of cottonsedge (*Eriophorum vaginatum*), various *Carex* sedge species, low shrubs (*Betula nana, Vaccinium uliginosum, Andromedra polifolia*), and mosses, predominantly *Sphagnum* sp.

The sandy sediments are interpreted as sand sheet deposits and alluvium, and they are adjacent to the Great Kobuk Sand Dunes (Mann et al. 2002). This study area was not glaciated at the time of the last

glacial maximum (Péwé 1975), but the ice wedges there are nonetheless interpreted to be Holocene epigenetic wedges, with minor syngenesis linked to Holocene peat accumulation. Thermokarst features indicative of large syngenetic ice wedges are lacking in the immediate study area. The lakes in the Ahnewetut Wetlands are sandy bottomed with relatively stable, vegetated shorelines. Most of the land between the lakes does not show outlines from the former shores of drained lakes, in contrast to the Lower Noatak Lowlands study area.

The southeast edge of the Ahnewetut Wetlands study area was burned by a lightning-caused wildfire in 1971 (Alaska Fire Service 2014). Just 7 of our 300 plots are both within the fire perimeter and cloud-free, and of these only two had visible ice-wedge polygons, so no comprehensive test of this fire's effect on ice-wedge polygons was possible.

Lower Noatak Lowlands, Noatak National Preserve

The Noatak National Preserve (NOAT) occupies 26,500 square kilometers of the lowlands along the Noatak River and adjacent mountains (Fig. 4). Ice-wedge polygons are common in the lowlands of NOAT, but visible polygons occur mostly in patches of 1 km^2 or less; the exception is the Lower Noatak Lowlands subsection (Fig. 7; Jorgenson et al. 2002). The Lower Noatak Lowlands (LNL) is a region of numerous thermokarst lakes and overlapping drained lake basins, with visible ice-wedge polygons on most of the land surface except recently drained lake basins (Fig. 8). The LNL is in the southwestern part of NOAT, which has the Preserve's warmest climate, and vegetation is a mix of boreal forest and arctic tundra. This area was selected for analysis because the density of ice-wedge polygons made sampling practical, and the relatively warm conditions presumably makes ground ice there particularly vulnerable in a warming climate.

Fourteen soil pits that were dug in polygon terrain in the Lower Noatak Lowlands as a part of another study (Swanson 2013) in early August 2013 showed frozen soil within 50 cm of the soil surface and free water perched above the frozen soil in all cases. The surface organic layer was 20 to 45 cm thick in 13 of the pits and over 45 cm thick but unknown (due to frozen soil) in one. The underlying mineral soil consisted of silt loam, probably lacustrine sediment. Vegetation was cottonsedge (*Eriophorum vaginatum*), various *Carex* sedge species, and low shrubs from the family *Ericaceae* (*Vaccinium uliginosum, Vaccinium vitis-idaea, Andromedra polifolia*), and mosses, predominantly *Sphagnum* sp. White spruce (*Picea glauca*) forest is present on well-drained soils of the Noatak River floodplain to the west of the study area.

The LNL is underlain mostly by lacustrine deposits of uncertain Holocene to Late Pleistocene age (Hamilton 2010). While thermokarst is ubiquitous across the LNL, indicating ice-rich ground, the thermokarst depressions have relatively low relief of just a few meters. Outlines of drained lakes cover most of the LNL, indicating reworking of the surface by thermokarst in the Holocene. Thus here, as in the Ahnewetut Wetlands study area, the ice wedges are interpreted to be Holocene epigenetic wedges, with minor syngenesis linked to Holocene peat accumulation.

The southern half of the Lower Noatak Lowlands was burned by a lightning-caused wildfire in 1977 (Alaska Fire Service 2014). Of our 300 LNL plots, 159 were within the fire perimeter, allowing us to test the effect of this fire on ice-wedge polygon stability.

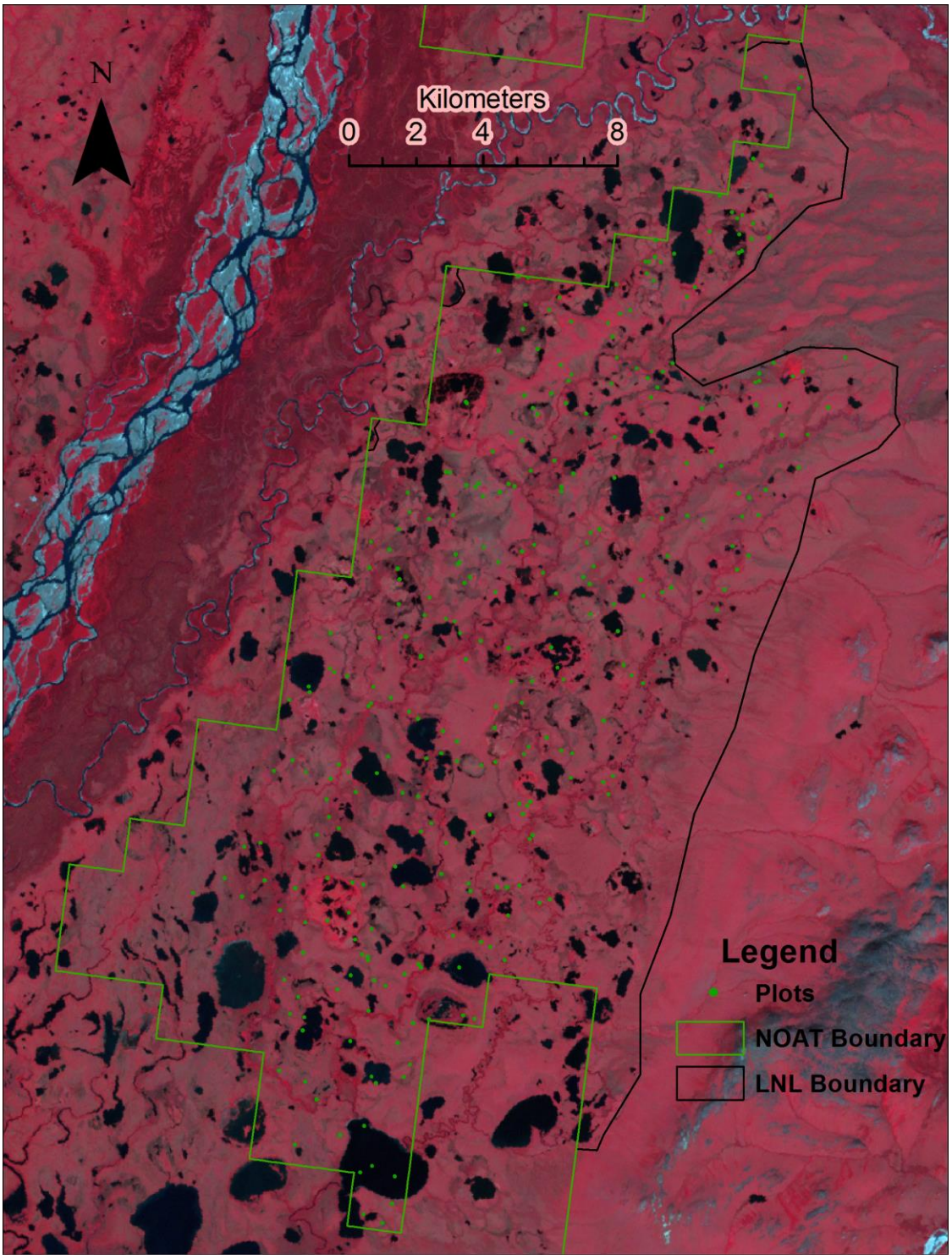

Figure 7. Overview of the Lower Noatak Lowlands study area. Remotely sensed plot locations are marked with green dots. The Noatak National Preserve boundary is show in green and the Lower Noatak Lowlands (LNL) boundary in the Preserve is shown in black. Portions of the LNL without plots were omitted due to lack of 1950s-era aerial photographs. The background image here is a Landsat mosaic from the early 2000s, displayed in a color-infrared color scheme.

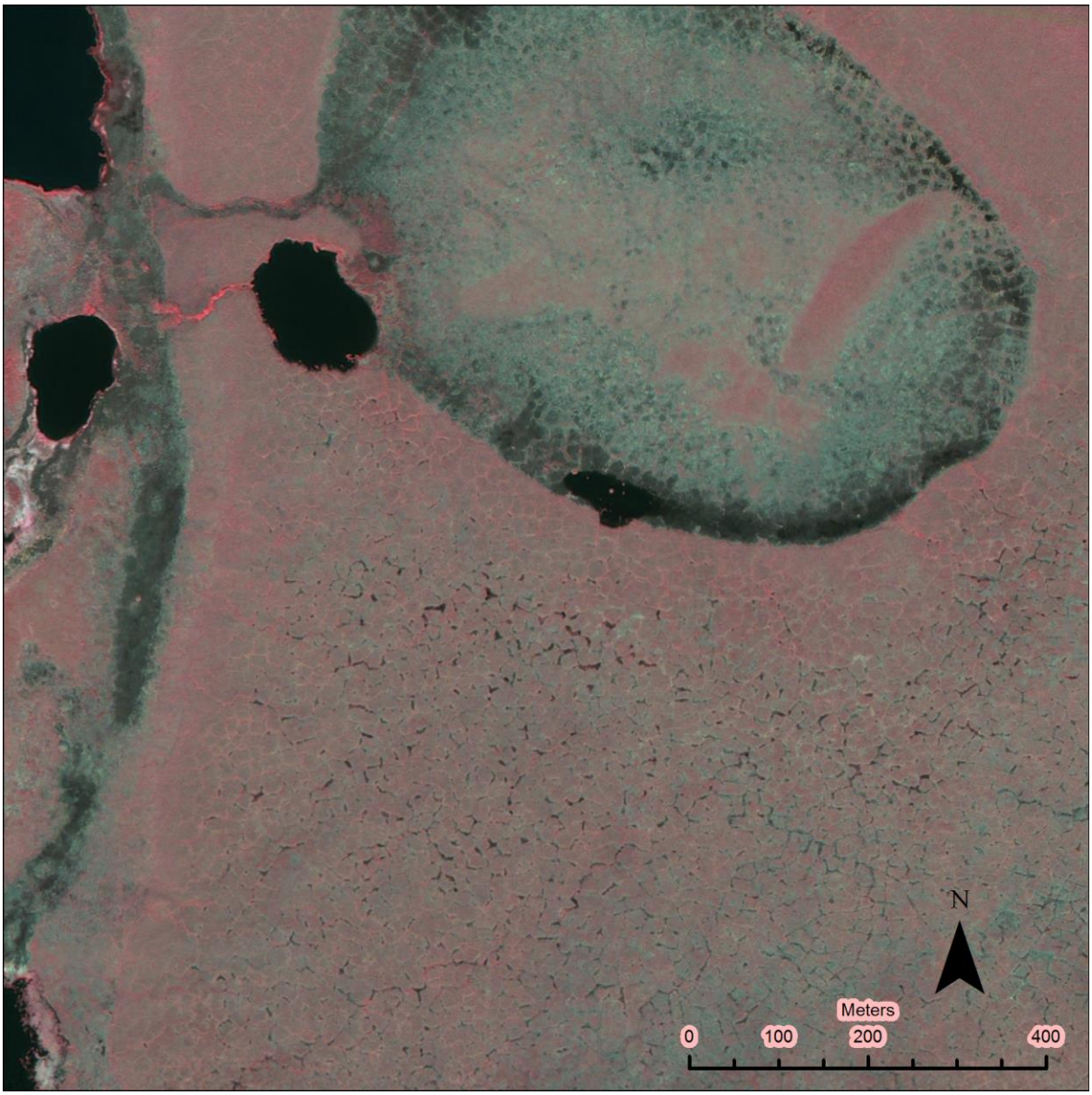

Figure 8. Landscape of the Lower Noatak Lowlands study area. A drained lake with low-center polygons is visible in the northern part of this IKONOS image (3 July 2007). Numerous ponds due to degradation of ice wedges are visible in the southern half of the image. A large drained lake with remnant smaller lakes is visible along the western edge of the image.

Climate

Long-term climate records are available for Kotzebue, about 175 km west of the AHN study area and 70 km south of the LNL study area. The running mean annual air temperature (computed monthly for the preceding year) at Kotzebue has fluctuated with a range of 4° C to 5° C in periods of just a few years (Fig. 9). The most obvious change over time was a shift to generally warmer conditions that occurred between 1976 and 1977, part of a statewide change (Hartmann and Wendler 2005). The mean annual air temperature at Kotzebue was -6.4° C prior to 1977 and -5.0° C after (Table 1). Trends before and after this stepwise shift were essentially flat: a seasonal Kendall test on monthly

mean temperature showed no significant trend from the start of continuous records in 1943 through 1976 (covariance-corrected p-value 0.65, slope -0.09° C/year) or from 1977 through 2009 (covariance-corrected p-value 0.87, slope 0.05° C/year). I ended the analysis in 2009 because this is our last image date, and thus this analysis does not include the recent (post-2012) warm peak. The seasonal Kendall test is a non-parametric test for monotonic trend that corrects for seasonal variations and serial autocorrelation (Hirsch and Slack 1984, Marchetto 2015.)

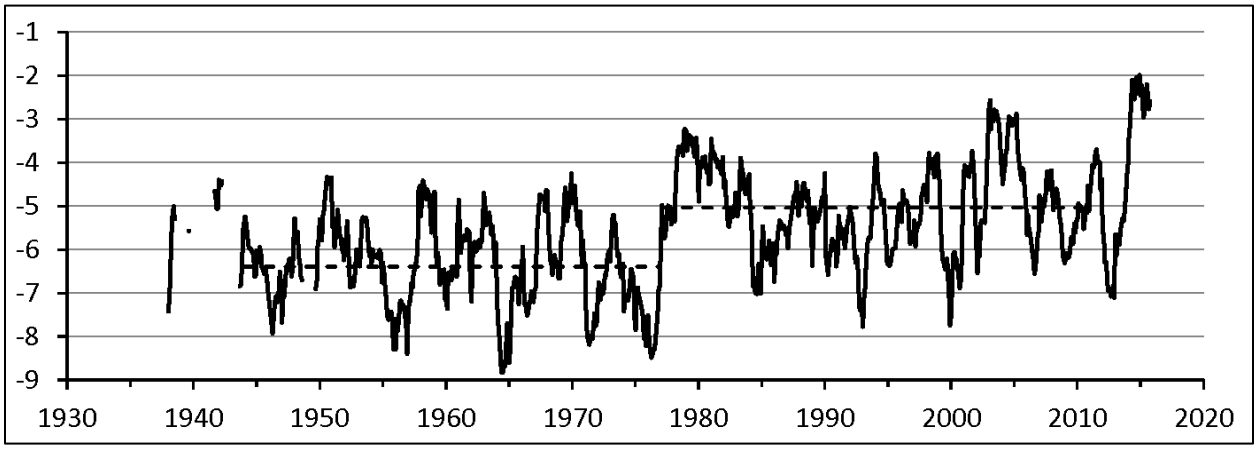

Figure 9. Running mean annual temperature at Kotzebue, Alaska. Means were computed monthly for the preceding 12 months. The dashed lines show the 1943-1976 and 1977-2009 means.

Table 1. Kotzebue mean monthly and annual temperature, 1943-1976 and 1977-2009[1]

Years	Jan	Feb	Mar	Apr	May	Jun	Jul	Aug	Sep	Oct	Nov	Dec	Ann
1943 to 1976	-20.4	-21.2	-18.4	-11.2	-0.7	6.2	11.7	10.4	5.2	-4.8	-13.6	-19.9	-6.4
1977 to 2009	-18.5	-18.1	-17.1	-10.4	0.1	7.7	12.8	11.1	5.7	-4.3	-12.6	-16.9	-5.0

[1]National Weather Service data, stored and processed by ACIS (http://xmacis.rcc-acis.org/)

The study areas have a more continental climate than Kotzebue, with colder winters and warmer springs and summer (Tables 2 and 3). The mean annual air temperature in the Ahnewetut Wetlands is about half a degree higher than Kotzebue, while the Lower Noatak Lowlands have a mean annual air temperature that is about half a degree lower than Kotzebue (Tables 2 and 3).

The annual sums of thaw degree-days were estimated for the two study areas using the mean monthly temperatures from Kotzebue and the average monthly corrections for the two study areas listed in Table 2 (Fig. 10). The annual sum of thaw degree-days is closely related to active-layer depth (Hinkel and Nicholas 1995, Nelson et al 1997). As in the case of mean annual air temperature, the main feature is a stepwise shift in 1976: from a mean of 1394° C-days through 1976 to 1533° C-days after at AHN, and 1148° C-days through 1976 to 1286° C-days after at LNL. Note that after the 1976-77 shift the estimated annual sum of thaw degree-days at the LNL was still lower than AHN's sum prior to the shift.

Table 2. Difference in mean monthly temperature between stations near the study areas and Kotzebue

Location	Jan	Feb	Mar	Apr	May	Jun	Jul	Aug	Sep	Oct	Nov	Dec	Ann
Kavet Cr[1]	-3.6	-0.1	1.6	3.6	5.0	5.8	2.3	0.2	-0.7	-1.5	-3.5	-3.2	0.5
Kotzebue 25N[2]	-3.0	-2.0	-0.8	1.1	2.4	3.7	0.5	-0.9	-1.5	-2.7	-2.8	-3.2	-0.8

[1]Kavet Creek is about 10 km west of the AHN and at similar elevation (latitude 67.1386°, longitude -159.0436°). Differences were computed for available monthly mean data, June 1992 through October 2015, with multiple gaps. Data for Kavet Creek from a Remote Automated Weather Station (RAWS) stored at http://www.raws.dri.edu/wraws/akF.html, and for Kotzebue, National Weather Service data, stored and processed by ACIS (http://xmacis.rcc-acis.org/)

[2]Kotzebue 25N is about 20 km south of the LNL and at similar elevation (latitude 67.25°, longitude -162.80°). Differences were computed for available monthly mean data, November 1982 through May 1995. National Weather Service data, stored and processed by ACIS (http://xmacis.rcc-acis.org/)

Table 3. Modeled average temperatures in the study area: January, July, and Annual[1]

Location	January	July	Annual
Kotzebue	-19.0	12.5	-5.5
AHN	-21.4 to -21.6	15.0 to 15.1	-5.0
Kavet Creek	-21.5	15.1	-4.9
LNL	-19.3 to -20.0	12.0 to 12.3	-5.8 to -5.9
Kotzebue 25N	-19.2	12.7	-5.8

[1]Modeling by the PRISM Climate Group (2009) for the period 1971-2000.

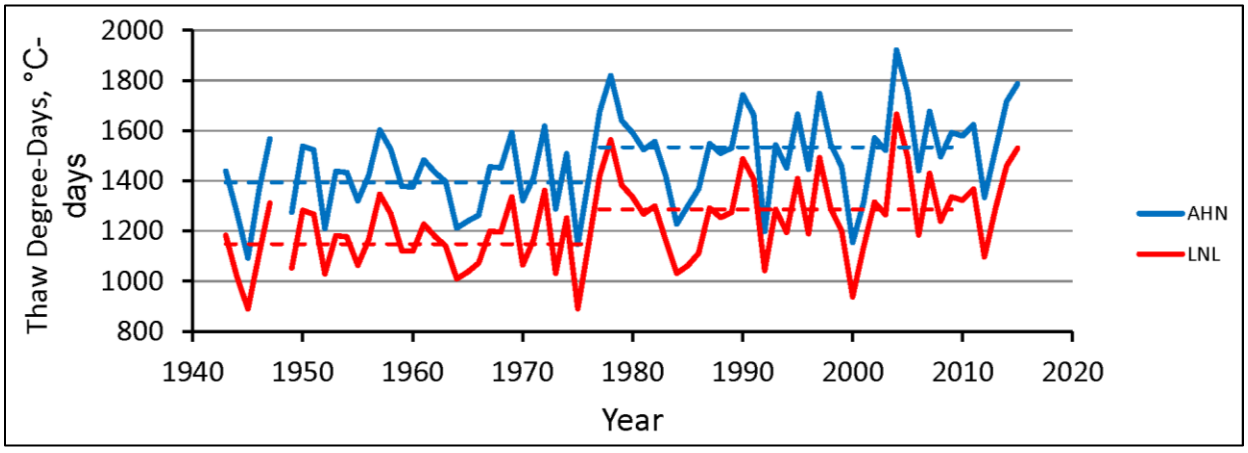

Figure 10. Time series of estimated annual sum of thaw degree-days at the two study areas. The sums were estimated using long-term temperature data from Kotzebue, corrected with the month-by-month differentials between Kotzebue and the two stations with shorter-term records (Table 2): Kavet Creek (for the AHN) and Kotzebue 25N (for the LNL).

Analytical Methods

Historical Aerial Photograph Preparation

Most of the Ahnetwetut Wetlands and Lower Noatak Lowland were covered by panchromatic aerial photographs with film scale of approximately 1:20,000, taken in 1951 or 1952. The photo dates were 25-26 Aug 1951 and 27 Aug 1952 for the Ahnewetut Wetlands and 15 July 1951 for the Lower Noatak Lowlands. They were scanned by the US Geological Survey EROS Data Center at 1800 dpi (14 microns). Scans were georeferenced to the IKONOS satellite images (described below) using ArcGIS 10.2 software with a perspective transformation and at least 10 control points per photo. The total root mean square error of each set of control points was less than 1 m, and no control point with greater than 2 m error was accepted. In this region of nearly flat topography, a perspective transformation yielded acceptable results without orthorectification. The corrected photos were resampled to 1 m resolution (matching the IKONOS imagery) by bilinear interpolation. The corrected photos were joined into a mosaic where overlap areas were displayed using the photo with the nearest center. The mosaic footprint layer (a layer of polygons designating which photo is displayed in overlap areas) was used to choose the best photo to sample for each plot. I corrected all of the available photos, which had approximately 60% overlap, so sampling was restricted to near the center of each photo, where spatial distortion and vignetting (the tendency for corners of photos to be darker) were minimized.

IKONOS Image Preparation

The recent condition of ice wedges in the study area was studied on IKONOS high-resolution satellite images. NPS has nearly complete coverage of the northern Alaska National Park units acquired in 2006 through 2009. The image dates were 20 Sept 2006, 10 Aug 2007, and 30 Sept 2009 for the Ahnetwetut Wetlands study area and 4 Sept 2006, 3 and 6 July 2007, and 8 July 2008 for the Lower Noatak Lowlands study area. This is 4-band color-infrared imagery with 4-m resolution, pan-sharpened to 1 m resolution. It was orthorectified using the manufacturer's satellite parameters and the 60 m National Elevation Dataset digital elevation model. To match the panchromatic air photos, I created an 8-bit (256 illumination levels) panchromatic satellite image by combining the red, green, and blue bands with equal weights. The mosaic footprint layer was again used to choose the best (cloud-free) image for sampling in overlap areas.

Plot Establishment

Within each study area I generated 300 randomly located circular 1-ha plots (radius 56.42 m). In the Ahnewetut Wetlands the area of the constraining feature for random plots was 141.9 km^2. I sampled the plots in random order, discarding those that were unsuitable due to lack of imagery, clouds, cloud shadows, or extensive tree shadows (which would be mistakenly mapped as water; 4 plots). I continued until 300 had been sampled, and in the process an additional 40 plots were discarded.

In the Lower Noatak Lowlands, both image dates were cloud-free and lacked significant tree shadows. The Lower Noatak Lowlands Subsection was clipped to the limits of available imagery and the NOAT boundary before generation of random plots. Thus all plots were suitable for sampling and the first 300 were sampled. The area of the constraining feature for the random plots was 586 km^2.

Identification of Ice-Wedge Polygon Zones

Within each plot I digitized a point at the center of every ice-wedge polygon that was visible on either image date. I also digitized ice-wedge polygon center points outside but within 30 m of the plot boundaries. The area encompassed by ice-wedge polygons within the plots was then outlined using the ArcGIS "Aggregate Points" geoprocessing tool, which connected the ice-wedge polygons centers closer than a chosen distance (30 m) and created a GIS polygon from the outermost of these lines. This process was chosen over similar "convex hull" procedures because it successfully created concave GIS polygons containing ice-wedges, surrounding areas without ice-wedges. The 30 m distance was chosen because this is approximately the maximum diameter of ice-wedge polygons. The resulting areas were clipped to the circular plot boundaries and are referred to as "ice-wedge polygon zones" (Fig. 11).

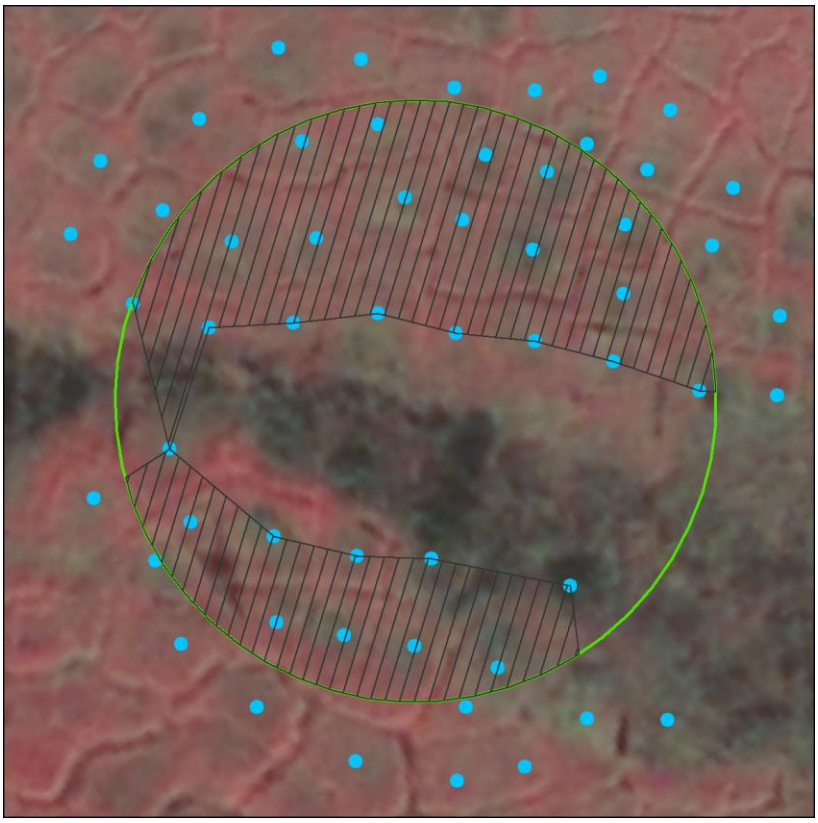

Figure 11. Example sample plot with digitized ice-wedge polygon centers and the ice-wedge polygon zone. The green circle is the one-hectare (56.42 m radius) sample plot. The "ice-wedge polygon zone" (hatched area) within the plot was created using the ArcGIS "Aggregate Points" geoprocessing tool, which connected the ice-wedge polygons centers (blue dots) closer than a chosen distance (30 m) and created a GIS polygon from the outermost of these lines.

Most of the 1-ha plots were only partly occupied by polygons (or lacked them entirely). Thus the plots represent samples of different sizes, and I chose to aggregate them for analysis, treating them as a single sub-area that is representative of the whole.

Mapping of Ice-Wedge Polygon Pits and Ponds

Water-filled pits and ponds were mapped by thresholding the panchromatic images (Jorgenson et al 2006, Liljedahl et al. 2016). Water bodies are the main dark-colored feature on the images, and thus a map of water bodies can be made by choosing a threshold pixel darkness and classifying all darker pixels as "water" and lighter pixels as "land". Thresholds were chosen manually for each image, with special attention to the ice-wedge zones and their vicinities; obvious water bodies outside the zones were also helpful as guides. The resulting binary raster maps (water vs. land) were clipped to the ice-wedge zone boundaries within the plots.

Water bodies within the ice-wedge zones are shallow and often have gently sloping margins with emergent vegetation; this makes differentiation of land and water difficult. As a result, a range of reasonable choices of thresholds can yield estimates of water area in ice-wedge zones that vary by a factor of almost two. For this reason, I chose the threshold for each image to produce what I judged subjectively to be the best possible map of water bodies, but I did not rely on the simple area of water to determine if ice wedges had degraded. The location of water bodies relative to polygon centers and margins was much less sensitive to the choice of thresholds, and thus my analysis is based on position of water bodies relative to polygon centers and not the area of water alone.

Compute and Analyze the Position Index of Water Pixels

A point was created at the center of each mapped water pixel, and the distance to the two closest ice-wedge polygon centers was determined using the ArcGIS "Generate Near Table" geoprocessing tool. The position index of each water pixel was then computed by the formula $2a/(a + b)$, where a is the distance from the center of the pixel to the closest ice-wedge polygon center and b is the distance to the second closest ice-wedge polygon center (Fig. 12). This index is known to community ecologists as the Sørenson distance index (McCune et al. 2002) and it ranges from near 0 at the polygon centers (where a is small and b relatively large) to near 1 along polygon boundaries (where a and b are approximately equal). The index was also computed for 10,000 random points in the ice-wedge zones of both study areas. In both study areas the distance indices for the 10,000 random points were 0.56, 0.75, and 0.89 for the 25^{th}, 50^{th}, and 75^{th} quantiles, respectively. Thus half of all random points had distance indices greater than 0.75. The reason for a preponderance of large distance indices is that the distance index approximates a radial distance measure, and area increases with the square of radius. The quantile breaks were used to define "quarter sectors" of the polygons. Thus all water pixels with indices between 0 and 0.56 were considered part of quarter sector 1, the innermost one-fourth of the polygons; pixels with an index of 0.56 to 0.75 were assigned to quarter sector 2 (just outside sector 1), and so on (Fig. 13)

The differences in the distribution of distance indices for water pixels between the two image dates, and between plots inside vs. outside the fire perimeter at LNL, were tested using the Wilcoxon Rank Sum test with continuity correction (the "wilcox.test" function in R statistical software; R Core Team 2014).

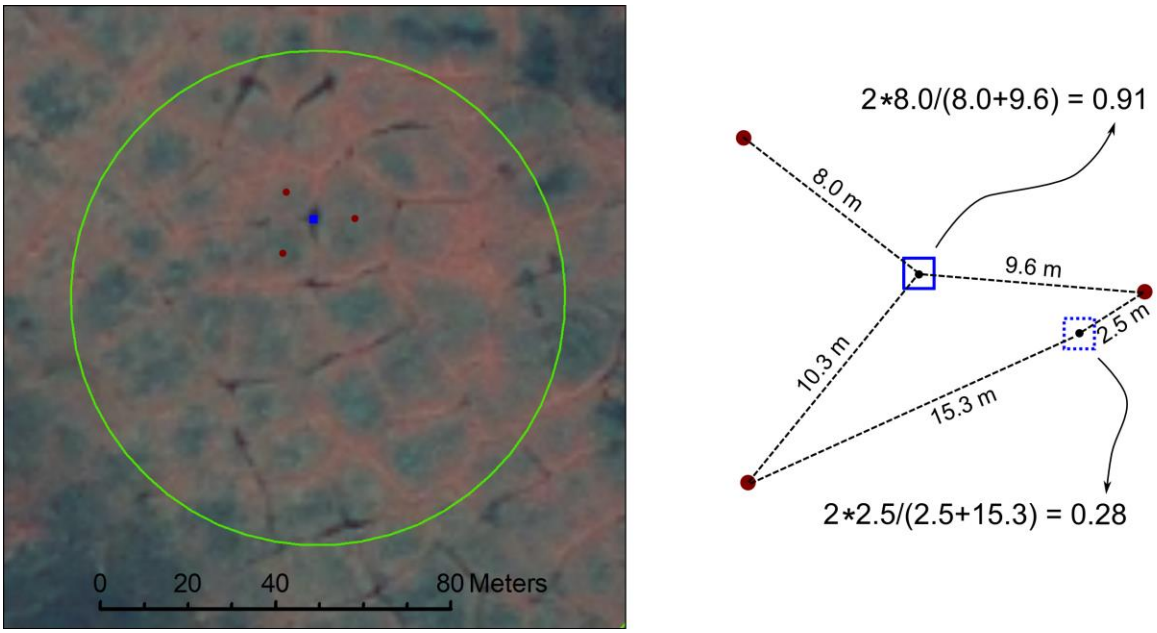

Figure 12. Computation of the water pixel position index. On the left is an example plot (plot 63 in AHN) with an example water pixel in blue on the polygon margins and three neighboring ice-wedge polygon centers. On the right, these features are magnified and the distance index is computed for this pixel (solid blue square) and a hypothetical pixel near one of the polygon centers (dotted blue square). The solid blue pixel near the polygon margins has a distance index of 0.91, while the dashed pixel near the right-most polygon center has an index of 0.28.

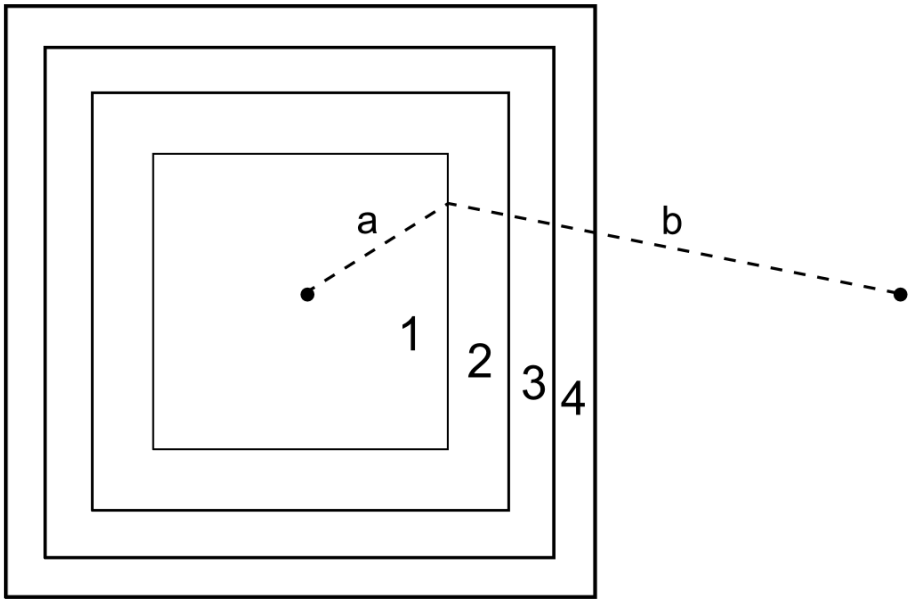

Figure 13. Sectors of polygons as defined by the distance index. The four numbered sectors of this schematic polygon have equal areas, each encompassing one-fourth of the area. The distance index i = 2a/(a + b) determines the boundaries of each sector. Distance indices were computed for 10,000 random points in the ice-wedge polygons of each of the two study areas to determine the boundaries between quarter sectors, and the resulting boundaries were i = 0.56, 0.75, and 0.89 for both study areas.

Proportion of Polygons with Degraded Ice-Wedges

The proportion of polygons with degraded ice-wedges was estimated as follows. Water pixels in the marginal sectors (sectors 3 and 4 in Fig. 13) were tallied for each polygon center. Each water pixel was assigned to both its nearest and second-nearest polygon center, since a wedge and its resulting pond are on the shared boundary of the two nearest polygons. A polygon was then counted as "having marginal pond(s)" if at least 5 m^2 of water pixels in sectors 3 or 4 were present. The proportion of polygons with these marginal ponds then approximates the proportion of polygons with degraded ice wedges.

Visual Assessment of Ice-Wedge Polygons

I also made a visual classification of polygon type on each 1-ha plot, and a visual assessment of the presence or absence of water-filled pits along polygon margins in the plot. The polygons on each plot were classified as low-centered (more than two-thirds of polygons had dark-colored centers), high-centered (more than two-thirds of polygons had light-colored centers), or mixed (both dark- and light-centered polygons were present, neither dominant). Water-filled marginal pits were considered "present" if any were found along polygon margins in the 1-ha plot. I did not attempt a significance test of the visual classification data, because the plots are not each equivalent samples from the population: the area of the ice wedge zones within the plots varies widely, from not present to the full 1 ha.

Results

Ahnewetut Wetlands

Of the 300 sampled plots, 63 had visible ice-wedge polygons (i.e. 237 plots had no polygons visible on either image date), and there were 1183 ice-wedge polygon centers within the plots. The total area of ice-wedge polygons within the 300 ha of plots was 24.0 ha, or 8.0% of the plot areas.

The area of water mapped within the ice-wedge polygon zones of plots was 2950 m^2 (1.2% of the ice-wedge polygon area; Table 4) in 1951-52 and 2821 m^2 (1.2% of the ice-wedge polygon area) in 2006-09. My experience with adjusting thresholds for mapping water shows that the difference in water area between the two dates (129 m^2) is much smaller than the range of values that can be obtained using various reasonable choices for the threshold pixel darkness values for water vs. land.

The proportion of water area in the various quarter-sectors of the ice-wedge polygons differed greatly between the two image dates (Fig. 14). In 1951 surface water was preferentially concentrated in polygon centers: about 35% of the water area was in the inner quarter-sector of the polygons (sector 1 in Fig. 13, with distance index less than 0.56) and the proportion of water dropped steadily moving outward from the center to just 17% in the outer quarter-sector (sector 4 in Fig. 13). In 2006-9 the distribution of water was the opposite: just 14% of the water area was in the inner quarter-sector of the polygons, and the proportion increased steadily to 39% in the outer quarter-sector (Fig. 14).

The median distance index for all water pixels was 0.67 in 1951-52 and 0.85 in 2006-09 (Table 4). The two distributions differ significantly by the Wilcoxon rank sum test, with a probability value of less than 10^{-15} that they originate from the same population.

In 1951-52, 7% of the 1183 polygons had 5 m^2 or more of water mapped in sectors 3 and 4 (margins), while 22% did in 2006-09 (Table 4). These percentages approximate the proportion of polygons with substantial wedge degradation.

Two plots with ice-wedge polygons were inside the 1971 fire perimeter, and both showed wedge degradation, similar to many plots outside of the fire perimeter.

Table 4. Summary of ice-wedge polygon water mapping

Study area	Image Years	Water Area, %	Median Distance Index of Water Pixels[1]	Polygons with marginal ponds[2], %
AHN	1951-52	1.23	0.67	7
	2006-09	1.18	0.85	22
LNL	1951-52	0.72	0.76	9
	2006-09	0.76	0.81	12

[1]Computed from the distances to the two nearest polygon centers and ranging from 0 at polygon centers to 1 at margins (Fig. 12). The median distance index of 10,000 random points was 0.75.

[2]Defined as polygons with at least 5 m^2 of water mapped in the marginal sectors 3 or 4 (see Fig. 13).

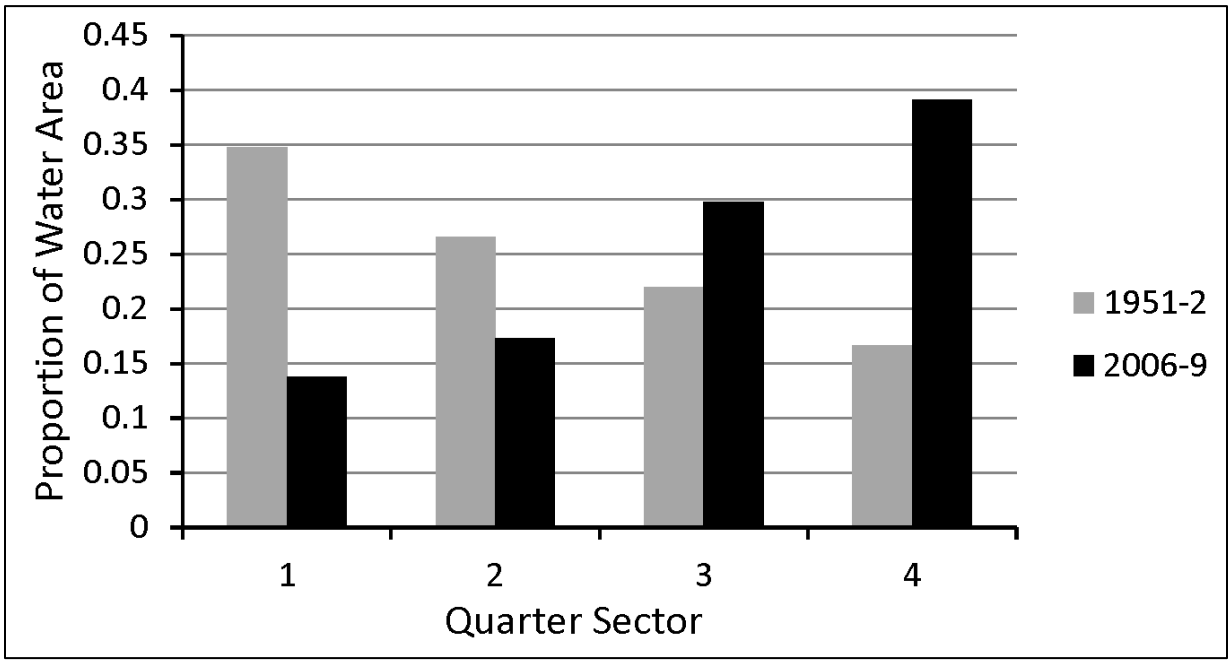

Figure 14. Proportion of mapped water area in four equal-area sectors of ice-wedge polygons, Ahnewetut Wetlands subsection. Each sector represents one quarter of the area in ice-wedges polygons, and they are numbered from 1 – polygon centers to 4 – polygon margins (Fig. 13).

Visual inspection of the plots showed that fewer plots in AHN had water-filled trenches on polygon margins in 1951-52 than 2006-09 (Fig. 15). New water-filled trenches in 2006-09 were common on all three polygon types (Table 5).

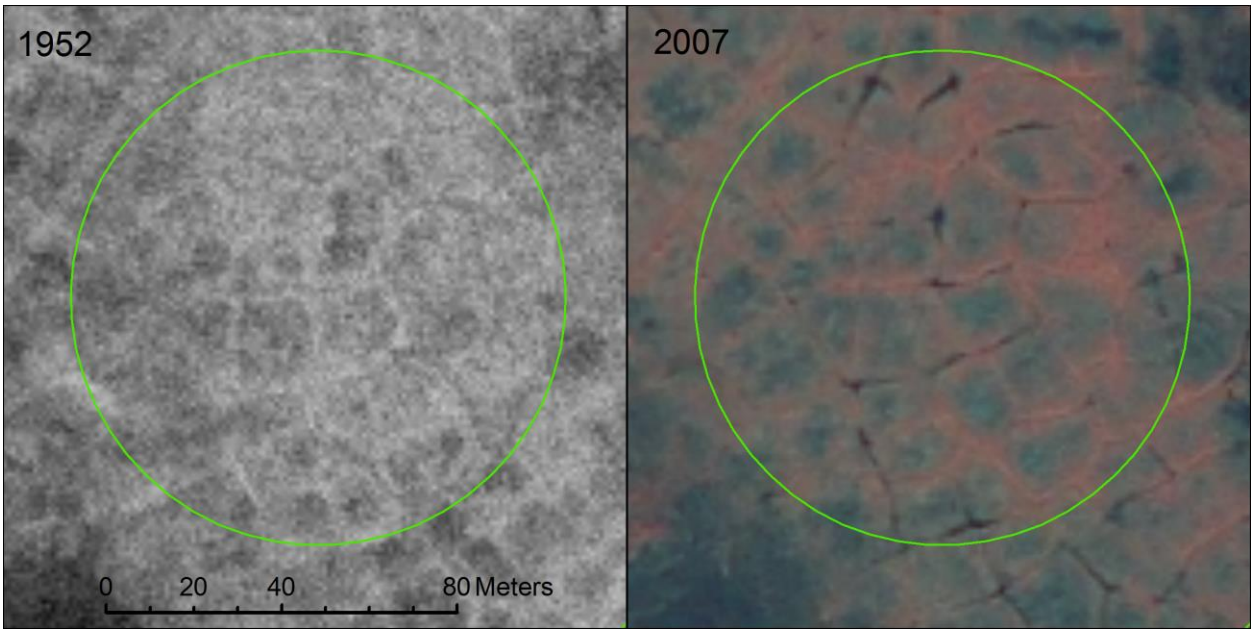

Figure 15. Example of ice-wedge degradation and pond formation, Ahnewetut Wetlands. The images are a panchromatic aerial photograph (left, 27 August 1952) and an IKONOS satellite image, color-infrared color scheme (right, 10 August 2007). Subsidence due to thaw of ice wedges between the image dates created water-filled trenches on the margins of these low-center polygons.

Table 5. Visual assessment of ice-wedge polygons sample plots

Study Area	Image Years	Plots with no Polygons	Count of plots with polygon-margin ponds/ count of all plots with polygons of that type[1]		
			Low-center	Mixed	High-Center
AHN	1951-52	238	0/6	10/25	0/31
AHN	2006-09	238	8/11	19/23	9/28
LNL	1951	175	2/16	20/50	19/61
LNL	2006-08	175	3/25	22/42	36/60

[1]The total count of plots was 300 at both localities and both dates. Low-center polygons: more than two-thirds of polygons had dark-colored centers, high-center: more than two-thirds of polygons had light-colored centers, mixed: both dark- and light-centered polygons present, neither dominant

Lower Noatak Lowlands

Of the 300 plots sampled in the LNL, 127 had visible ice-wedge polygons (i.e. 173 plots had no polygons visible on either image date). Polygons covered 66.3 ha (22.1% of the plot area), and there were 3207 ice-wedge polygon centers in the plots. The area of water mapped within the ice-wedge polygon zones of plots was 4757 m^2 (0.72% of the ice-wedge polygon area) in 1951 and 5053 m^2 (0.76% of the ice-wedge polygon area) in 2006-08. Again, this difference of 296 m^2 is smaller than the variability of results that could be obtained by choosing various reasonable threshold values to map water on the images.

The proportion of the surface water in the various sectors of the ice-wedge polygons differed between the two image dates, but less strongly than in the Ahnewetut wetlands (Fig. 16). In 1951 the proportion of water in quarter-sector 1 (polygon centers) was similar to sectors 3 and 4 (polygon margins), with less in sector 2 (just outside the center). Thus surface water was present in both low polygon centers and in marginal troughs. In 2006-08 sector 2 was again the driest, but both marginal sectors had more water than the central sector (Fig. 16).

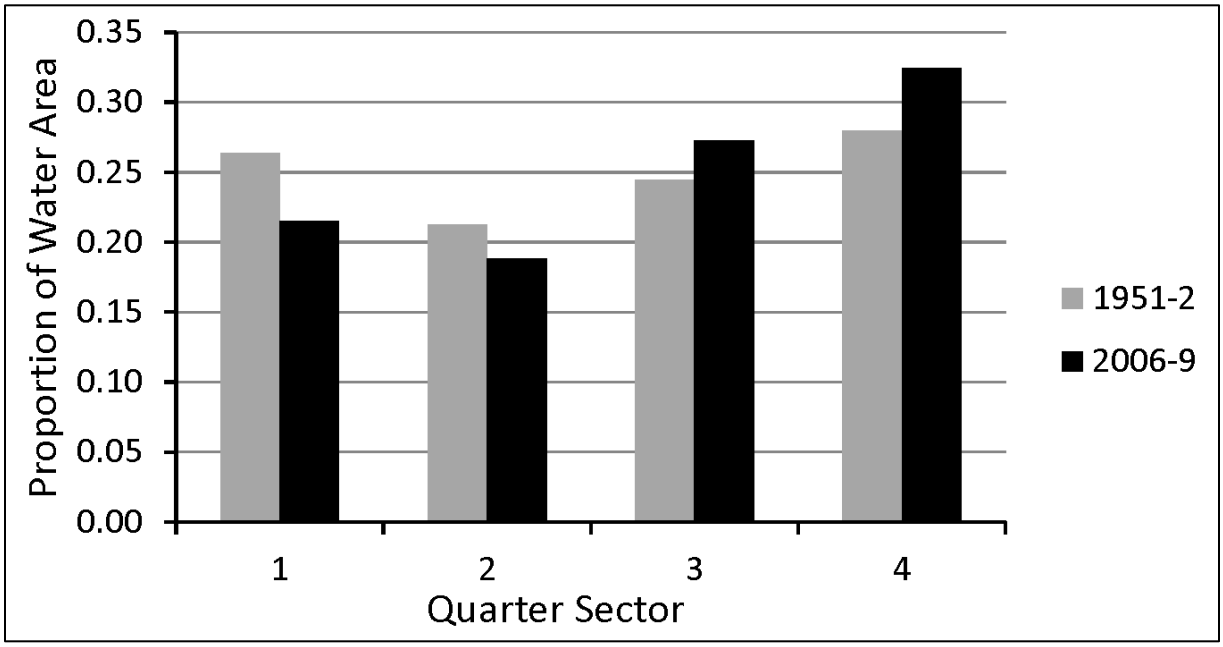

Figure 16. Proportion of mapped water area in four equal-area sectors of ice-wedge polygons, Lower Noatak Lowlands subsection. Each sector represents one quarter of the area in ice-wedges polygons, and they are numbered from 1 – polygon centers to 4 – polygon margins.

The median distance index for all water pixels was 0.76 in 1951-52 and 0.81 in 2006-09. These two distributions differ significantly by the Wilcoxon rank sum test, with a probability value of 10^{-13}. Thus the water was located significantly more along polygon margins at the later sample date, but the difference was less marked than at AHN.

In 1951, 9% of 3207 polygons had 5 m^2 or more of water mapped in sectors 3 and 4 (the margins), while 12% did in 2006-08 (Table 4). Thus more polygons had marginal ponds at the later date, but the difference between the dates was again less marked than at AHN.

The area of water mapped in the burned area of the LNL study area dropped from 0.91% to 0.40%, while in the unburned area it increased from 0.53% to 1.09%. However, the distance indices of the water pixels inside and outside of the burn area did not differ, and both the burned and unburned areas showed a similar (and significant) change between years (Table 6).

Table 6. Effect of 1977 fire on distance index of water in the Lower Noatak Lowlands study area

Treatment	Median Distance Index of Water Pixels		Wilcoxon Test p-value[1]
	1951-52	2006-09	
No burn	0.76	0.81	**10^{-8}**
1977 burn	0.77	0.82	**10^{-6}**
Wilcoxon Test p-value[2]	**0.21**	**0.20**	--

[1]Wilcoxon Rank-Sum Test, the probability that the two groups of distance indices on this row were drawn from the same distribution

[2]Wilcoxon Rank-Sum Test, the probability that the two groups of distance indices in this column were drawn from the same distribution

Visual inspection of the plots showed that water-filled trenches along polygon boundaries were present on both dates. Some of the trenches visible in 1951-2 were still visible in 2006-9, while others had healed, and new ones formed (Fig. 17). New polygon marginal troughs were most common in high-center ice-wedge polygon areas (Table 5). The wettest areas, dominated by low-center polygons, had few polygon-marginal ponds on either date (Table 5). Figure 8 shows an example of this situation: the drained lake basin in the northern part of the image is quite wet and has intact low-center polygons, while the better drained area to the south with a mix of high- and low-center polygons has numerous polygon-marginal ponds.

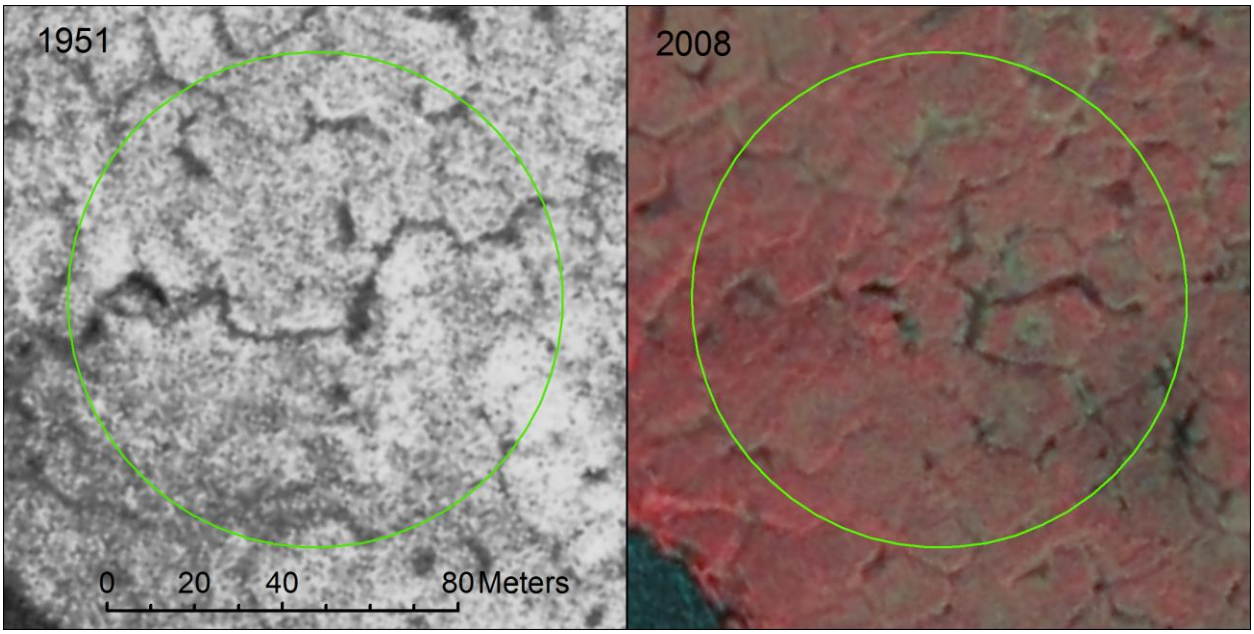

Figure 17. Example of ice-wedge changes in the Lower Noatak Lowlands. The images are a panchromatic aerial photograph (left, 14 July 1951) and an IKONOS satellite image, color-infrared color scheme (right, 8 August 2008). Water-filled trenches are present on the margins of these high-center and flat polygons at both dates. Note that some of the ponds present in 1951 became less prominent by 2008 while others formed, resulting in no clear net gain or loss. Between the two image dates, the lake in the southwest corner of the scene expanded about 10 m toward the plot by permafrost thaw subsidence and bank erosion.

Discussion

The Ahnewetut Wetlands ice wedge polygons are the southeastern-most extensive field of ice-wedge polygons in this part of Alaska, suggesting that climatic conditions were marginal for ice wedge growth even before recent climate warming. The 1976-77 climate shift in the region probably resulted in deeper active layers and thaw of some of the ice wedges. The numerous polygon-margin pits visible in 2006-09 were not visible on July 1978 aerial photographs of AHN, confirming that the pits indeed developed after the 1976-77 climate shift, though exactly when they formed between 1978 and 2006-09 is unknown. (I chose not to quantitatively analyze the 1978 aerial photographs because of their lower resolution than the 1951-52 photos and 2006-09 IKONOS images.) Necsoiu et al. (2013) also observed that ice-wedge degradation in their small study area within the Ahnetwetut Wetlands occurred after the 1978 photos were taken. Large ground-ice bodies are apparently not present in the AHN, because thermokarst has not continued to develop beyond small elongate ponds on ice-wedge polygon margins.

The different history of ice-wedge degradation in the LNL study areas probably results from its slightly different climate and geologic setting, but the specific causes are not clear. The 1976-77 climatic shift occurred in the LNL too, but its effects appear to have been less marked than at AHN. It is possible that, with mean annual air temperatures in the LNL roughly a degree colder than at AHN and the annual sum of thaw degree-days about 200°C-days less, polygons were able to, at least in part, stabilize after adjusting to the deeper post-1976 active layer. Jorgenson et al. (2015) have shown how degraded ice wedges can become the locus of plant growth and peat accumulation, which in turn facilitate ground ice aggradation and heave, and ultimately reduce the marginal ponds. Also, much of the polygon terrain in the LNL is very wet former lake basins, which appear to be more resistant to degradation (e.g. Fig. 8). Jorgenson et al. (2006) also noted less dramatic ice-wedge degradation in very wet lowlands on the North Slope of Alaska.

Some water-filled marginal troughs were present in both study areas in 1951-52. Frost et al. (2015) noted similar ponds at their study areas on the western North Slope of Alaska in the 1950s. These could represent "normal" polygon development, in which occasional local ponding of water produces positive feedback on ground temperatures (by absorbing solar energy) and consequent local thermokarst. It could also be a response to warming from the cold "Little Ice Age" conditions of the late 1800s to warmer conditions that peaked around 1940 before leveling off (IPCC 2014). If we accept the 1950s as "normal" conditions of the era before the late-19th century warming, then the presence of marginal ponds on 7% (AHN) to 9% (LNL) of polygons would be our standard for polygons prior to impacts due to warming.

Fire effects.

Based on the distribution of ponds inside and outside of the 1977 fire perimeter at LNL, the fire did not significantly enhance ice-wedge degradation. Wedge degradation due to the Anaktuvuk River fire of 2007 was reported by Jones et al. (2015), but on terrain different from the LNL. In the Anaktuvuk River fire area, troughs from degrading wedges appeared after the fire on gently sloping upland slopes where polygons were not visible before. Apparently in the very wet soils of the LNL, the 1977

fire did not consume sufficient organic matter to cause enhanced wedge degradation, or if it did, peat infilled the resulting troughs during the intervening years. My sample size of just two plots within fire perimeters at AHN was too small to draw any conclusions about fire effects on ice wedges there.

Comparison to other studies.

Ice-wedge degradation in my two study areas is similar to what has been described in other recent studies (Jorgenson et al. 2006, Raynolds et al. 2014, Frost et al. 2015, Liljedahl et al. 2016). These studies also reported degradation commencing as a result of late 20th-century warming, with troughs forming over a period of a decade or two. Degradation appears more dramatic in the other studies, perhaps because these researchers deliberately chose sites with degraded wedges in order to study degradation processes, or at least emphasized the results from areas with dramatic change. My sampling scheme of random plots placed across an entire physiographic unit known to contain polygons was designed specifically to provide an objective landscape-wide assessment of polygon degradation.

Limitations of remote sensing.

Remote sensing has several limitations as a method for detecting changes in ice-wedge polygons. Water is used as a proxy for topography to detect subsidence due to melt of ice wedges. Unfortunately, the amount of water on the landscape changes through time as a result of the season and weather, and these changes could be mistaken for changes in polygon microtopography. In addition, differences in image type and quality between dates could result in different areas of water mapped. Also, over long time periods, growth of vegetation and peat accumulation could obscure or fill shallow ponds. These limitations lead especially to errors in the total area of water mapped. Thus I analyzed the position of water relative to polygon centers, reasoning that even if the above problems caused inconsistencies between dates in the total area of water mapped, a change in position of ponds between polygon centers and margins was likely to be caused by true microtopographic changes.

Implications for the ecosystem.

An increase in thermokarst due to ice-wedge degradation could have profound effects on the ecosystem, as changes in microtopography affect the area and depth of water bodies, and alter surface drainage, soil processes, and vegetation. While ice-wedge degradation has definitely occurred in my two study areas, the effects of appear to be minor thus far. The net change in pond area due to wedge degradation was below the detection capability of my methods, and in both study areas the resulting thermokarst depressions have not enlarged beyond small polygon-margin ponds a meter or two wide and several meters long. The surfaces occupied by polygons in the Ahnetwetut Wetlands study area are well above the level of lakes, and hence channels formed by wedge degradation do not appear to be capable of causing lake drainage. No lake drainage events have been noted in recent decades in the AHN study area (Swanson 2013). In the thaw-lake plain terrain of the LNL study area, on the other hand, much of the difference in elevation between lake bottoms and adjacent land is due to ground ice, and ice-wedge degradation could lead to lake drainage. Three lake drainage events have been documented in the LNL since 1979, and ice wedge degradation may have been a factor. However, the total area of surface water in the LNL has remained fairly constant over the past 35

years (Swanson 2013). The relatively modest rate of ice-wedge degradation here has probably helped make this relative lake stability possible.

Prospects for the future.

Mean annual air temperatures at the Kavet Creek monitoring station near AHN during 2013-2015 have been about -2 °C, well above the long-term average and marginally cold enough to maintain permafrost (Swanson 2016). These warm temperatures should cause ice-wedge degradation to continue in the AHN. With additional warming above -2 °C, all permafrost in AHN would become thermally unstable and all ice wedges would degrade, resulting in high-center polygons (Fig. 18) across most of the polygonal terrain in AHN. Based on my plot sampling, ice-wedge polygons cover about 8% of the Ahnewetut Wetlands ecological subsection, which covers about 142 km^2 (Swanson 2001). Ice wedges without visible surface manifestation are probably also present, and thus more than 8% of the area is likely to be affected if all wedges degrade. Because of the apparently limited ice content of these sediments, thermokarst effects here should be limited to a meter or so of subsidence along polygon margins. More severe thermokarst is likely in other parts of KOVA with more ice-rich, silty sediments (e.g., the Nigeruk Plain subsection, Swanson 2001); but lack of visible polygons there made analysis like the one presented here impossible.

Figure 18. A high-center ice-wedge polygon in the Ahnewetut Wetlands study area. Ponds have formed over degraded ice wedges around the entire perimeter of this polygon.

Temperatures in Kotzebue since 2013 have also been well above long-term averages: about -2.5 °C (Fig. 9) which translates to -3 to -3.5 °C at LNL. If these warm temperatures continue they would represent a climatic shift larger than the one that occurred in the 1970s and would likely result in deepening of the active layer and renewed ice-wedge degradation in the LNL. The lower mean annual temperatures at LNL provide a slightly greater margin before permafrost in general becomes unstable with warming. But according to modeling by scientists from the University of Alaska Geophysical Institute's Permafrost Laboratory (Panda, Marchenko, and Romanovsky, unpublished), before the current century is over permafrost will become unstable in the LNL and pervasive ice-wedge degradation will occur. This will result in the formation of high-center polygons (especially on slightly higher surfaces) and also extensive thermokarst, including lake drainage, enlargement of existing lakes, and formation of new ponds.

Literature Cited

Alaska Fire Service. 2014. “Fire History in Alaska. Bureau of Land Management, Alaska Interagency Coordination Center.” http://afsmaps.blm.gov/imf_firehistory/imf.jsp?site=firehistory.

Cleland, David T., Peter E. Avers, W. Henry McNab, Mark E. Jensen, Robert G. Bailey, Thomas King, and Walter E. Russell. 1997. “National Hierarchical Framework of Ecological Units.” In *Ecosystem Management Applications for Sustainable Forest and Wildlife Resources*, edited by M. S. Boyce and A. Haney, 181–200. New Haven, CT: Yale University.

Cohen, K. M., S. C. Finney, P. L. Gibbard, and J.-X. Fan. 2013. “The ICS International Chronostratigraphic Chart.” *Episodes* 36 (3): 199–204.

Czudek, Tadeáš, and Jaromir Demek. 1970. “Thermokarst in Siberia and Its Influence on the Development of Lowland Relief.” *Quaternary Research* 1 (1): 103–20.

Frost, G., M. J. Macander, A. K. Liljedahl, and D. A. Walker. 2015. “Regional Patterns of Ice-Wedge Degradation Across Northern Alaska: What Does Asynchronous Timing of Onset Tell Us Regarding Triggering Mechanisms, Thresholds, and Impacts?” In *2015 AGU Fall Meeting*. AGU. https://agu.confex.com/agu/fm15/webprogram/Paper61659.html.

Hamilton, Thomas Dudley. 2010. “Surficial Geologic Map of the Noatak National Preserve, Alaska.” http://pubs.usgs.gov/sim/3036/.

Hartmann, Brian, and Gerd Wendler. 2005. “The Significance of the 1976 Pacific Climate Shift in the Climatology of Alaska.” *Journal of Climate* 18 (22): 4824–39.

Hinkel, Kenneth M., and James RJ Nicholas. 1995. “Active Layer Thaw Rate at a Boreal Forest Site in Central Alaska, USA.” *Arctic and Alpine Research* 27 (1): 72–80.

Hisch, Robert M., and James R. Slack. 1984. “A Nonparametric Trend Test for Seasonal Data with Serial Dependence.” https://profile.usgs.gov/myscience/upload_folder/ci2012Oct1508284428033A%20Nonparametric%20Trend%20Test%20for%20Seasonal%20Data%20With%20Serial%20Dependence.pdf.

IPCC. 2014. “Climate Change 2014: Synthesis Report. Contribution of Working Groups I, II and III to the Fifth Assessment Report of the Intergovernmental Panel on Climate Change.” Geneva, Switzerland: IPCC. http://ipcc.ch/report/ar5/syr/.

Jones, B. M., G. Grosse, C. D. Arp, E. Miller, L. Liu, D. J. Hayes, and C. F. Larsen. 2015. “Recent Arctic Tundra Fire Initiates Widespread Thermokarst Development.” *Scientific Reports* 5: 15865. doi:10.1038/srep15865.

Jorgenson, M. T., M. Kanevskiy, Y. Shur, N. Moskalenko, D. R. N. Brown, K. Wickland, R. Striegl, and J. Koch. 2015. “Role of Ground Ice Dynamics and Ecological Feedbacks in Recent Ice

Wedge Degradation and Stabilization." *Journal of Geophysical Research: Earth Surface* 120 (11): 2280–97.

Jorgenson, M. Torre, Yuri L. Shur, and Erik R. Pullman. 2006. "Abrupt Increase in Permafrost Degradation in Arctic Alaska." *Geophysical Research Letters* 33 (2). http://onlinelibrary.wiley.com/doi/10.1029/2005GL024960/pdf.

Jorgenson, M. Torre, David K. Swanson, and Matt Macander. 2002. *Landscape-Level Mapping of Ecological Units for the Noatak National Preserve, Alaska*. ABR, Incorporated–Environmental Research & Services.

Jorgenson, M. T., K. Yoshikawa, M. Kanevskiy, Y. Shur, V. Romanovsky, S. Marchenko, G. Grosse, J. Brown, and B. Jones. 2008. "Permafrost Characteristics of Alaska." Fairbanks, Alaska: Institute of Northern Engineering, University of Alaska Fairbanks. http://www.cryosphericconnection.org/resources/alaska_permafrost_map_dec2008.pdf.

Lachenbruch, A. H. 1963. "Contraction Theory of Ice-Wedge Polygons: A Qualitative Discussion in." In *Proceedings, Permafrost International Conference:*, 63–71. Washington, D.C.: National Academy of Sciences, National Research Council. http://www.arlis.org/docs/vol1/ICOP/.

Leffingwell, E. de K. 1915. "Ground-Ice Wedges: The Dominant Form of Ground-Ice on the North Coast of Alaska." *The Journal of Geology*, 635–54.

Liljedahl, A. K., J. Boike, R. P. Daanen, A. N. Fedorov, G. V. Frost, G. Grosse, L. D. Hinzman, et al. 2016. "Pan-Arctic Ice-Wedge Degradation in Warming Permafrost and Its Influence on Tundra Hydrology." *Nature Geoscience*. doi:10.1038/NGEO2674.

Mann, D. H., P. A. Heiser, and B. P. Finney. 2002. "Holocene History of the Great Kobuk Sand Dunes, Northwestern Alaska." *Quaternary Science Reviews* 21 (4): 709–31.

Marchetto, Aldo. 2015. *Rkt: Mann-Kendall Test, Seasonal and Regional Kendall Tests. R Package Version 1.4*. http://CRAN.R-project.org/package=rkt.

McCune, Bruce, James B. Grace, and Dean L. Urban. 2002. *Analysis of Ecological Communities*. Vol. 28. Gleneden Beach (OR): MjM software design. http://www.researchgate.net/profile/James_Grace/publication/216769990_Analysis_of_ecological_communities/links/0a85e5318e69b2ae7f000000.pdf.

Necsoiu, M., C. L. Dinwiddie, G. R. Walter, A. Larsen, and S. A. Stothoff. 2013. "Multi-Temporal Image Analysis of Historical Aerial Photographs and Recent Satellite Imagery Reveals Evolution of Water Body Surface Area and Polygonal Terrain Morphology in Kobuk Valley National Park, Alaska." *Environmental Research Letters* 8 (2): 025007.

Nelson, F. E., N. I. Shiklomanov, G. R. Mueller, K. M. Hinkel, D. A. Walker, and J. G. Bockheim. 1997. "Estimating Active-Layer Thickness over a Large Region: Kuparuk River Basin, Alaska, USA." *Arctic and Alpine Research* 29 (4): 367–78.

Péwé, Troy Lewis. 1975. “Quaternary Geology of Alaska.” US Govt. Print. Off.,. https://pubs.er.usgs.gov/publication/pp835.

PRISM Climate Group. 2009. “July Mean Average Temperature for Alaska 1971-2000; Annual Mean Average Temperature for Alaska 1971-2000. Corvallis (OR): Oregon State University.” http://prism.oregonstate.edu.

R Core Team. 2014. “R: A Language and Environment for Statistical Computing.” Vienna, Austria: R Foundation for Statistical Computing. http://www.R-project.org.

Raynolds, M. K., D. A. Walker, K. J. Ambrosius, J. Brown, K. R. Everett, M. Kanevskiy, G. P. Kofinas, V. E. Romanovsky, Y. Shur, and P. J. Webber. 2014. “Cumulative Geoecological Effects of 62 Years of Infrastructure and Climate Change in Ice-Rich Permafrost Landscapes, Prudhoe Bay Oilfield, Alaska.” *Global Change Biology* 20 (4): 1211–1224.

Romanovskiy, N. N. 1977. *Formirovaniye polygonal’no-zhilnykh struktur*. Novisibirsk: Nauka, Sibirskoye Otdeleniye.

Shur, Y., M. Z. Kanevskiy, M. T. Jorgenson, D. Fortier, M. Dillon, E. Stephani, and M. Bray. 2009. “Yedoma and Thermokarst in the Northern Part of Seward Peninsula, Alaska.” In *AGU Fall Meeting Abstracts*, C41:0443. http://adsabs.harvard.edu/abs/2009AGUFM.C41A0443S.

Swanson, D. K. 2001. “Ecological Units of Kobuk Valley National Park, Alaska.” Anchorage, Alaska: National Park Service. https://irma.nps.gov/App/Reference/Profile/584437.

———. 2013. “Surface Water Area Change in the Arctic Network of National Parks, Alaska, 1985-2011: Analysis of Landsat Data.” NPS/ARCN/NRDS—2013/445. Natural Resource Data Series. Fort Collins, Colorado. https://irma.nps.gov/App/Reference/Profile/2193078.

———. 2015. “Vegetation Sampling in the Arctic Inventory and Monitoring Network, 2013 Progress Report.” NPS/ARCN/NRDS—2013/580. Natural Resource Data Series. Fort Collins (CO). Accessed June 15. https://irma.nps.gov/App/Reference/Profile/2204497.

———. 2016. “Soil Temperatures in Alaska’s Arctic National Parks, 2011-2015, and Implications for Permafrost Stability.” Natural Resource Report NPS/ARCN/NRR—2016/1109. Fort Collins, Colorado: National Park Service. https://irma.nps.gov/DataStore/Reference/Profile/2226036.

van Everdingen, Robert O. 1998. *Multi-Language Glossary of Permafrost and Related Ground-Ice Terms in Chinese, English, French, German, Icelandic, Italian, Norwegian, Polish, Romanian, Russian, Spanish, and Swedish*. Boulder, CO: International Permafrost Association, Terminology Working Group, National Snow and Ice Data Center. http://nsidc.org/fgdc/glossary/.

The Department of the Interior protects and manages the nation's natural resources and cultural heritage; provides scientific and other information about those resources; and honors its special responsibilities to American Indians, Alaska Natives, and affiliated Island Communities.

NPS 187/133533, 189/133533, July 2016

National Park Service
U.S. Department of the Interior

Natural Resource Stewardship and Science
1201 Oakridge Drive, Suite 150
Fort Collins, CO 80525

www.nature.nps.gov

2016 National Park Service CENTENNIAL

EXPERIENCE YOUR AMERICA ™